Physics of Fluids

Splashing of liquid droplet on a vibrating substrate

Cite as: Phys. Fluids **32**, 122109 (2020); https://doi.org/10.1063/5.0033409
Submitted: 15 October 2020 . Accepted: 25 November 2020 . Published Online: 09 December 2020

T. I. Khabakhpasheva, and A. A. Korobkin

Physics of Fluids ARTICLE scitation.org/journal/phf

Splashing of liquid droplet on a vibrating substrate

Cite as: Phys. Fluids 32, 122109 (2020); doi: 10.1063/5.0033409
Submitted: 15 October 2020 • Accepted: 25 November 2020 •
Published Online: 9 December 2020

T. I. Khabakhpasheva[1,a] and A. A. Korobkin[1,2,b]

AFFILIATIONS

[1] Lavrentyev Institute of Hydrodynamics, pr. Lavrentyeva 15, Novosibirsk 630090, Russia
[2] University of East Anglia, Norwich NR4 7TJ, United Kingdom

[a] Author to whom correspondence should be addressed: tana@hydro.nsc.ru
[b] Electronic mail: a.korobkin@uea.ac.uk

ABSTRACT

The unsteady axisymmetric problem of a liquid drop impacting onto a rigid vibrating substrate is studied. Initially, the drop is spherical and touches the flat substrate at a single point. Then, the substrate starts to move toward the drop and vibrate with a small amplitude and high frequency. The early stage of the impact is studied by using the potential flow theory and the Wagner approach in dimensionless variables. The effect of the substrate vibration on the drop impact is described by a single parameter. It is shown that the vibration of the substrate leads to oscillations of the pressure in the contact region. The low-pressure zone periodically appears in the wetted part of the substrate. The low-pressure zone can approach the contact line, which may lead to ventilation with separation of the liquid from the substrate. The magnitude of the low pressure grows in time. The acceleration of the contact line oscillates with time, leading to splashing of the droplet with the local increase of the thickness of the spray jet sheet at a distance from the contact line. The phase shift of the substrate vibration with respect to the impact instant is not studied. Splashing can be produced only by a forced vibration of the substrate. The impact onto an elastically supported rigid plate does not produce splashing. The obtained results and the theoretical model of the initial stage of drop impact are valid for certain ranges of parameters of the problem.

I. INTRODUCTION

Liquid drop impact onto a rigid or elastic substrate and the subsequent splashing is a fascinating phenomenon that is still difficult to describe and to understand [see Rein (1993) and Yarin (2006)]. Splashing occurs when a droplet hits a substrate and does not spread on the substrate smoothly but produces small droplets and jets, which scatter from the substrate. Splashing depends on the liquid of the droplet, velocity of impact, size of the droplet, properties of the substrate, and presence of a gas around the droplet. It is challenging to predict splashing and to reveal the dominant underlying mechanisms. Splashing is important in many industrial and environmental fields, ranging from microfluidics to agriculture. In some applications, such as fuel combustion, splashing is beneficial, while in others, it has adverse effects, such as pesticide delivery onto plant leaves, where splashing should be minimized. Splashing is difficult to study, either experimentally, theoretically, or numerically. The splashing behavior is set at very early times after, or possibly just before, impact, far before the actual splash occurs [see Pepper *et al.* (2008)]. Splashing can be suppressed by using elastic membranes with controlled (reduced) tension (Courbin *et al.*, 2006). The problem of drop impact on elastic and compliant surfaces is still under investigation (Chen, 2005). Drop impact onto an elastic plate with high flexural rigidity may induce or trigger high-frequency vibration of the plate leading to vibration of the drop, its splashing, and even atomization (James *et al.*, 2003 and Pegg *et al.*, 2018). The problem of wave impact onto elastic structures was intensively studied in marine and offshore hydrodynamics [see Faltinsen (2000), Korobkin (1998), Korobkin *et al.* (2008), and Korobkin and Khabakhpasheva (2006)] with the focus on stresses in the structures and the hydrodynamic loads.

The dynamic behavior of a sessile droplet sitting on a vibrating elastic plate was investigated by Tsai *et al.* (2015). The characteristics of the droplet oscillation were studied experimentally by using two high-speed cameras recording side and top views synchronously. Theoretical dynamic shapes of the droplet and

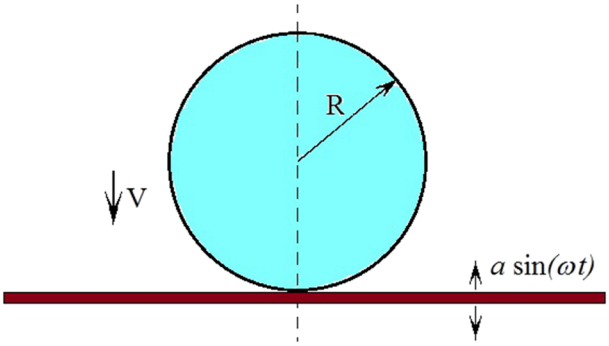

FIG. 1. Initial position of the droplet before impact.

frequencies of its oscillations were compared with those measured in the experiments, and different regimes of the droplet oscillations were explained. Moreover, the circular patterns of the elastic plate vibrations were visualized. The radii of the nodal lines on the plate as functions of the frequency of the external forcing were well predicted by a theoretical model. A droplet placed at a nodal line oscillates due to the pitch motion of the plate at this line but not due to the plate vertical vibration that is negligible at the nodal line. A droplet located either outside or inside the nodal lines behaves differently, resulting in potential depinning of the contact line due to the gradient of the plate deflection. The contact line is either stationary or moves periodically in time depending on the plate frequency and its amplitude.

Pegg *et al.* (2018) studied an early stage of a spherical liquid drop impact onto a rigid substrate with a small built-in elastic circular plate. The impact forced the elastic plate to vibrate, which changed the expansion rate of the wetted part of the substrate and the parameters of the spray sheet that emanates from the periphery of the wetted region. As a result, the velocity of the spray sheet oscillated, leading to breaking the sheet with consequent splashing and lifting the liquid in the sheet from the substrate. This type of splashing happens in the inertia-dominated regime, when surface tension, the viscosity of the liquid, gravity, and the presence of gas in the place of the impact play minor roles.

The present study of a liquid drop impact on a vibrating rigid plate is related to both the problem of drop impact on an elastic substrate and the problem of a sessile droplet on a vibrating plate (Fig. 1). Forced vibration of the plate can produce a layer of cavitating liquid near the impact region if the frequency of the plate vibration is high enough. Such a cavitating layer significantly changes spreading and possible splashing of the droplet. It is possible that the liquid starts to cavitate near the impact region even before the drop touches the substrate due the presence of air between the droplet and the substrate. The presence of air is not taken into account in this study, which could correspond to the impact inside a chamber without a gas in it. Zones of low pressures on the vibrating plate and oscillation of the expanding contact line may also enhance splashing and could prevent wetting of the substrate. The present study is focused on the early stage of the impact, duration of which is comparable with the period of the plate vibration. The radius of the wetted part of the plate is much smaller than the droplet radius during this stage. The large-time behavior of a droplet impacting a vibrating substrate was studied experimentally by James *et al.* (2003) and numerically by Moradi *et al.* (2020). We are concerned with the initial stage and conditions of droplet impact, where the impact effects and vibrations effects are comparable. The axisymmetric problem of liquid drop impact is investigated under the assumption of large Reynolds and Weber numbers by using methods of asymptotic analysis.

II. FORMULATION OF THE PROBLEM

Initially, the drop is spherical with radius R. The plate touches the free surface of the droplet at a single point taken as the origin of the cylindrical coordinate system r, z. It is convenient to invert the problem and consider the plate impact onto the droplet [see Fig. 2(a) for the initial configuration and Fig. 2(b) for the sketch of the axisymmetric flow just after the impact] with an oscillating velocity $-V - a\omega\cos(\omega t)$, where V is the mean velocity of the plate, a is the amplitude of the plate vibration, and ω is the frequency of the vibration. The current position of the plate is given by the equation $z = -[Vt + a\sin(\omega t)]$ [see Fig. 2(b)]. Surface tension, viscosity of the liquid, and gravity play minor roles during the early stage of the impact. During this stage of impact, the flow region is approximately divided into the main region, the jet root region at the periphery of the wetted part of the vibrating plate, and the jet sheet itself [see Fig. 2(c)]. The flow in the main region is studied by using the potential flow theory and the Wagner approach [see Wagner (1932), Korobkin and Pukhnachov (1988), and Howison *et al.* (1991)].

In this approach, the flow near the impact place is governed by Laplace's equation for the velocity potential $\varphi(r, z, t)$ with the main flow region being approximated by the lower half-space,

$$\nabla^2\varphi = 0 \qquad (z < 0). \tag{1}$$

The boundary conditions in the contact region and on the free surface of the droplet are linearized and imposed at the initial position

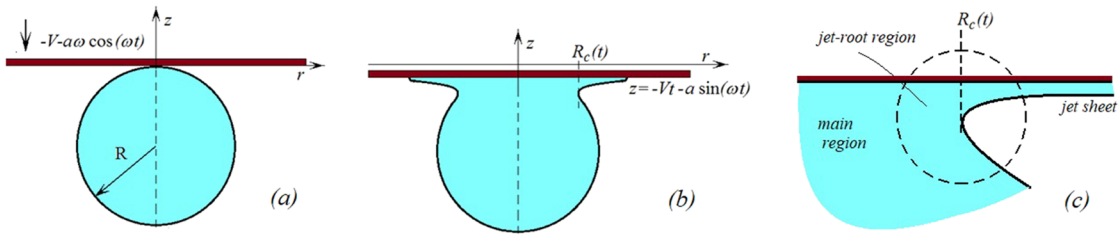

FIG. 2. Sketch of the plate impact onto the droplet. (a) Initial configuration. (b) Deformation of the drop during the impact. (c) Asymptotic decomposition of the flow region.

of the plate, $z = 0$ [see Howison *et al.* (1991)]. The dynamic condition on the free surface reads

$$\varphi(r, 0, t) = 0 \qquad (z = 0,\ r > R_c(t)), \tag{2}$$

and the linearized boundary condition in the wetted part of the plate is

$$\frac{\partial \varphi}{\partial z} = -V - a\omega \cos(\omega t) \qquad (z = 0,\ r < R_c(t)), \tag{3}$$

where the mean velocity of the plate V and the amplitude of the velocity of the plate vibration, $a\omega$, are assumed to be of the same order. The velocity potential is required to decay in the far field,

$$\varphi \to 0 \qquad \left(z^2 + r^2 \to \infty\right), \tag{4}$$

which means that the flow induced by impact is localized near the impact place.

The radius of the contact region, $R_c(t)$, is unknown in advance and should be determined as part of the solution. It is defined as the radius of the line on the free surface, where the tangent to the free surface is normal to the surface of the plate [see Fig. 2(b)]. The shape of the free surface of the droplet is determined approximately by using the linearized kinematic boundary condition, where $z = 0$ and $r > R_c(t)$. Within the Wagner theory, the radius $R_c(t)$ is obtained from the condition that the deformed free surface of the droplet at time t intersects the current position of the plate at $r = R_c(t)$. This additional condition is known as the Wagner condition.

Dimensionless variables are used below, where $1/\omega$ is the time scale, V is the velocity scale, and V/ω is the displacement scale. The length scale, $L = \sqrt{RV/\omega}$, is obtained by estimating the radius of the contact region from the geometrical consideration without account for deformation of the droplet during the early stage [see Pegg *et al.* (2018)]. If the length scale L is much smaller than the radius of the droplet R, then one can approximate the flow region by the half-space $z < 0$, and if it is much greater than the displacement scale, then one can approximately impose the boundary conditions at the initial position of the plate, $z = 0$, as in (2) and (3), when the parameter $\varepsilon = L/R = \sqrt{V/(\omega R)}$ is small. The problem is studied under the condition that the velocity of the plate vibration, $a\omega$, is of the same order but smaller than the mean velocity of the plate V. This condition introduces a parameter of the problem, $\mu = a\omega/V$, where $0 < \mu < 1$, $a = \varepsilon^2 \mu R$, and $\varepsilon \ll 1$. The dimensionless velocity potential $\tilde{\varphi}(\tilde{r}, \tilde{z}, \tau)$ is introduced by $\varphi(r, z, t) = VL\tilde{\varphi}(\tilde{r}, \tilde{z}, \tau)$, where VL is the scale of the velocity potential and $r = L\tilde{r}$, $z = L\tilde{z}$, and $\tau = \omega t$. Dimensionless variables are denoted with tilde. The dimensionless radius of the wetted part of the plate is $r_c(\tau) = R_c(t)/L$. The position of the plate in the dimensionless variables is described by the equation $\tilde{z} = -\varepsilon h(\tau)$, where $h(\tau) = \tau + \mu \sin \tau$. The dimensionless hydrodynamic pressure is given by the linearized Bernoulli equation $\tilde{p}(\tilde{r}, \tilde{z}, \tau) = -\partial \tilde{\varphi}/\partial \tau$ with the pressure scale $\rho V^2/\varepsilon$, where ρ is the liquid density. Tilde is dropped below.

III. PRESSURE DISTRIBUTION

The formulated problem is equivalent to that of a rigid paraboloid, $z = \varepsilon(r^2/2 - h(\tau))$, entering the liquid half-space, $z < 0$, at the oscillating speed $h'(\tau)$. The latter problem was solved in Sec. 7 of Korobkin and Scolan (2006). The velocity potential in the contact region, $z = 0$, $r < r_c(\tau)$, is given by

$$\varphi(r, 0, \tau) = -\frac{2}{\pi} h'(\tau) \sqrt{r_c^2(\tau) - r^2}, \qquad r_c(\tau) = \sqrt{3h(\tau)}. \tag{5}$$

The pressure distribution in the contact region reads

$$p(r, 0, \tau) = \frac{2}{\pi} \frac{G(r, \tau)}{\sqrt{r_c^2(\tau) - r^2}},$$
$$G(r, \tau) = -\mu \sin \tau (r_c^2(\tau) - r^2) + \frac{3}{2}(1 + \mu \cos \tau)^2. \tag{6}$$

The obtained pressure distribution shows that the pressure in the contact region is always positive close to the contact line, $r = r_c(\tau)$, and also everywhere in the contact region when $\sin \tau < 0$. When $\sin \tau > 0$, the function $G(r, \tau)$ is a monotonic function of r with its minimum value at $r = 0$, $G(0, \tau) = -3\mu(\tau + \mu \sin \tau) + \sin \tau + 3/2(1 + \mu \cos \tau)^2$. If $G(0, \tau) < 0$, there is a region $r < r_0(\tau)$, $r_0(\tau) < r_c(\tau)$, where the pressure is negative (below the atmospheric pressure) and the liquid may cavitate.

The pressure $p(r, 0, \tau)$ at the center of the contact region, $r = 0$, is shown in Fig. 3(a) for different values of the parameter μ. The pressure is singular at the impact instant,

$$p(0, 0, \tau) \sim \frac{\sqrt{3}}{\pi} \frac{(1 + \mu)^{\frac{3}{2}}}{\sqrt{\tau}} \qquad (\tau \to 0).$$

The pressure oscillates with time. The pressure magnitude grows as $O(\sqrt{\tau})$, and it is larger for larger μ. The pressure is well approximated by

$$p(0, 0, \tau) \approx p_{as}(0, 0, \tau) = -\frac{2\sqrt{3}}{\pi} \mu \sqrt{\tau} \sin \tau \tag{7}$$

after two periods of the plate vibration, $\tau > 4\pi$ [see Fig. 3(b)]. The regions of negative pressure in the contact region are shadowed in the plane (τ, μ) [see Fig. 3(c)]. The zone of negative pressure appears earlier for high-frequency oscillations (large μ) than for small frequencies.

The hydrodynamic force $F(t)$ acting on the vibrating plate due to the drop impact is given by $F(t) = F_0(t)N(\tau)$, where

$$F_0(t) = 2\rho V^2 (3R)^{3/2} \sqrt{Vt} \tag{8}$$

is the force acting on the stationary plate and the factor

$$N(\tau) = \sqrt{1 + \mu \frac{\sin \tau}{\tau}} \left(1 + \frac{1}{6}\mu^2 + 2\mu \cos \tau - \frac{2}{3}\mu\tau \sin \tau + \frac{5}{6}\mu^2 \cos(2\tau)\right) \tag{9}$$

describes the effect of the plate vibration on the hydrodynamic loads. The function $N(\tau)/\mu$ is shown in Fig. 3(d) for $\mu = 0.4$, 0.7, and 1 together with its large-time asymptotics,

$$\frac{1}{\mu} N_{as}(\tau) = \frac{2}{3}\tau \sin \tau. \tag{10}$$

It is seen that $N(\tau)$ oscillates with the amplitude, which grows linearly in time.

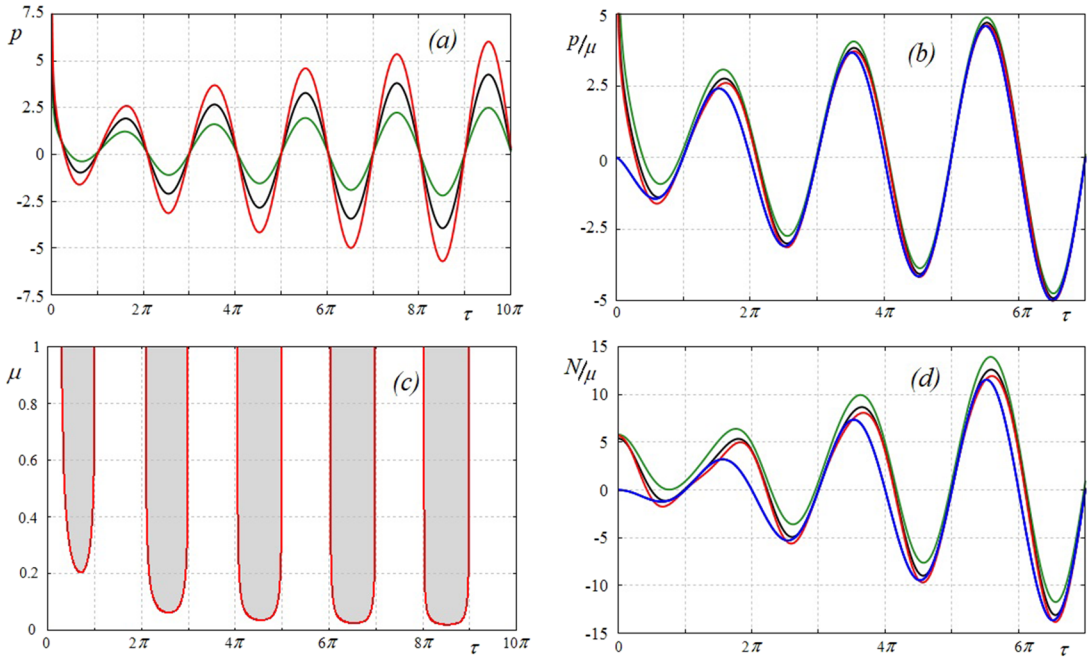

FIG. 3. (a) Pressures $p(0, 0, \tau)$ at the center of the wetted area for $\mu = 0.4$ (green line), 0.7 (black line), and 1 (red line) as functions of the dimensionless time τ. (b) Pressures $p(0, 0, \tau)/\mu$ for $\mu = 0.4$, 0.7, and 1 and the asymptotic pressure $p_{as}(0, 0, \tau)/\mu$ (blue line). (c) The regions of the plane (τ, μ), where the pressure $p(0, 0, \tau)$ is negative. (d) The functions $N(\tau)/\mu$ for $\mu = 0.4$, 0.7, 1, and $N_{as}(\tau)/\mu$ (blue line).

The liquid cavitates in the impact region [see Fig. 3(a)] if the total dimensional pressure $p_{atm} + \rho V^2 \varepsilon^{-1} p(0, 0, \tau)$ at the center of the impact region drops down to the vapor pressure p_{cav}. For room temperature and water droplets, we have $p_{cav} \approx 3$ kPa and $p_{atm} \approx 0.1$ MPa. The pressure scale for impact velocity $V = 2$ m/s, $\rho = 1000$ kg/m^3, and $\varepsilon = 0.1$ is 40 kPa. The total pressure drops to the vapor pressure then when $p(0, 0, \tau) < -2.4$. Figure 3(a) shows that the liquid cavitates, in particular, for $\mu = 0.7$ during the second period of the plate vibration. Note that the droplet does not bounce from the plate but continues to spread on the vibrating plate trapping the region of cavitating liquid. The conditions of the present calculations, $V = 2$ m/s, $\mu = 0.7$, and $\varepsilon = 0.1$, for a droplet of water of radius $R = 1$ mm imply the amplitude of the plate vibration $a = 7 \cdot 10^{-6}$ m and frequency $\omega = 2 \cdot 10^5$ s^{-1}.

The present approach is valid for $\epsilon \ll 1$, which means that the droplet displacement during the period of the plate vibration, V/ω, is much smaller than the radius of the droplet, and $0 < a\omega/V < 1$, which implies that the velocity of the plate vibration is of order of the impact velocity but does not exceed it. These conditions require a small amplitude of the plate vibration at a high frequency. See more details about the validity ranges of the present model in the Conclusion. According to Rayleigh's formula, the lowest oscillation frequency of the droplet of water of radius $R = 1$ mm and surface tension $\sigma = 0.0728$ N/m is equal to 763 Hz, which is two orders below the frequency range of this study. Therefore, we do not expect the resonance phenomenon when the frequency of the plate vibration is close to a natural frequency of the droplet.

IV. EVOLUTION OF THE SPRAY JET

The Wagner solution of the impact problem (1)–(4) is not valid close to the contact line, $r = r_c(\tau)$, where it predicts the square-root singular flow velocity and the pressure. Within the asymptotic theory of impact, a jet root region is introduced at the periphery of the wetted part of the rigid surface [see Pegg *et al.* (2018)]. The flow in the jet root region is quasi-stationary and nonlinear. The axisymmetric spray sheet is ejected from the jet root region in the radial direction with the dimensional velocity $2R_c'(t)$ and dimensional thickness $h_{j0}(t) = U^2(t)R_c(t)/[2\pi R_{c,t}^2(t)]$ [see Oliver (2002), Korobkin (1997), and Scolan and Korobkin (2003)], where $U = V + a\omega\cos(\omega t)$ is the velocity of impact including the velocity of the plate vibration. In the dimensionless variables, the jet speed is equal to

$$\frac{V}{\varepsilon}\frac{\sqrt{3}\,h'(\tau)}{\sqrt{h(\tau)}}, \tag{11}$$

and the jet thickness is given by

$$h_{j0}(\tau) = L\varepsilon^2 \frac{2}{\sqrt{3}\pi} h^{3/2}(\tau). \tag{12}$$

The spray jet caused by the drop impact is very thin, which makes it possible to neglect the hydrodynamic pressure in the jet at leading order as $\varepsilon \to 0$. The continuity equation for the spray sheet in the axisymmetric case was asymptotically integrated in Korobkin

(1997). The solution in the parametric form is

$$r = r_c(T)\left[\frac{h'(T)}{h(T)}(\tau - T) + 1\right], \qquad r_c(T) = \sqrt{3h(T)}, \tag{13}$$

$$h_j(r,\tau) = h_{j0}(T)\left|1 - 2\frac{r_c''(T)}{r_c'(T)}(\tau - T)\right|^{-1}\left|1 + 2\frac{r_c'(T)}{r_c(T)}(\tau - T)\right|^{-1}, \tag{14}$$

where T is the parameter equal to the dimensionless time at which a liquid particle enters the jet, $T < \tau$. In formula (14), always $r_c'(T) > 0$, but the dimensionless acceleration, $r_c''(T)$, of the contact line can be either negative or positive. Initially, where $0 < T < \pi$, the acceleration $r_c''(T)$ is negative, and the thickness of the jet head, where $0 < \tau < \pi$, is bounded. If $r_c''(\hat{T}) > 0$ later at a certain $\hat{T}$, then $h_j(r, \tau) \to \infty$ as $\tau \to \tau_c(\hat{T})$ [see (14)], where

$$\tau_c(\hat{T}) = \hat{T} + \frac{r_c'(\hat{T})}{2r_c''(\hat{T})}. \tag{15}$$

The minimum value of the function $\tau_c(\hat{T})$, where $\hat{T} \geq \pi$, defines the time instant τ_{c*} and the corresponding time T_{c*}, when the spray sheet thickness $h_j(r, \tau)$ becomes unbounded for the first time within the present asymptotic model of liquid drop impact. This blow-up occurs at $r = r_{c*}$, where

$$r_{c*} = r_c(T_{c*})\left[1 + \frac{[r_c'(T_{c*})]^2}{r_c(T_{c*})\, r_c''(T_{c*})}\right]. \tag{16}$$

In our problem,

$$\frac{r_c''(T)}{r_c'(T)} = \frac{2hh'' - (h')^2}{2hh'(T)}, \qquad h(T) = T + \mu \sin T,$$

which predicts positive accelerations of the contact line when

$$-2\mu \sin T > \frac{(1 + \mu \cos T)^2}{T + \mu \sin T}. \tag{17}$$

The regions in the plane (T, μ), where inequality (17) is satisfied, are shadowed in Fig. 4(a). The place on the spray sheet, $r_{c*}(\mu)$, where the jet thickness becomes unbounded for the first time and the time, $\tau_{c*}(\mu)$, when it happens, calculated using (15) for $\pi < T < 10\pi$, is shown in Fig. 4(b). For small frequencies (small μ), the jet blows up far from the contact region. For $0.2 < \mu < 1$, the jet thickness becomes unbounded within the first three periods of the plate oscillations. The discontinuous behavior of the function $\tau_{c*}(\mu)$, where $0 < \mu < 0.2$, is explained by Figs. 4(c) and 4(d), where the functions $r_{c*}(\mu)$ and $\tau_{c*}(\mu)$ are shown separately for the intervals $\pi < T_{c*} < 2\pi$, $3\pi < T_{c*} < 4\pi$, and $5\pi < T_{c*} < 6\pi$.

The evolution of the dimensionless jet thickness $h_j(r, \tau)$, which is given by (14), just before its first blow-up is shown in Fig. 5(a) for $\mu = 0.5$. The scale of the jet thickness is $L\varepsilon^2$ [see (12)]. The thickness of the spray jet increases beyond all bounds at a dimensionless distance of $r_{c*} = 3.9$ from the impact place, which produces a vertical splashing jet of corona type in this axisymmetric case. The evolution of the maximum thicknesses of the spray sheet as functions of time for several values of $\mu = a\omega/V$ is presented in Fig. 5(b). The blow-up of the jet sheet occurs later for smaller μ.

The evolution of the spray jet for $\mu = 0.2$ is shown in Fig. 6(a). The jet root solution, which smoothly matches the free surfaces in the main flow region and in the jet sheet, is not shown here. Several places with vertical jets emanated from the spray sheet may occur for smaller μ [see Fig. 6(b) for $\mu = 0.05$].

The plate vibration may lead to an unbounded increase of the spray sheet thickness. This phenomenon can be associated either

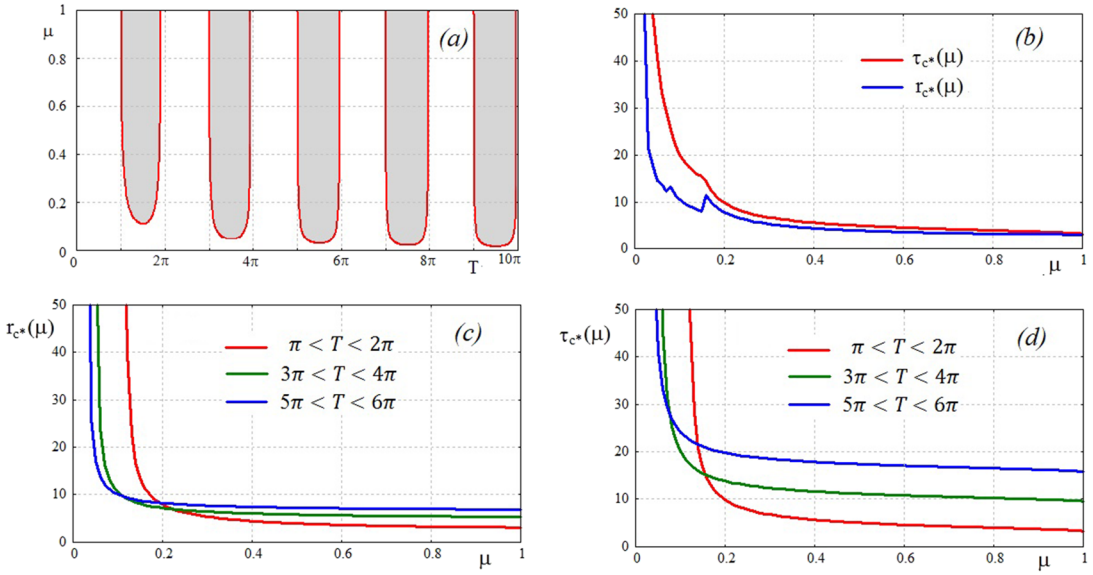

FIG. 4. (a) Regions of positive accelerations of the contact line are shadowed in the plane (T, μ). (b) The radial distance $r_{c*}(\mu)$ (blue line) and the time $\tau_{c*}(\mu)$ (red line) of blow-up. (c) The function $r_{c*}(\mu)$ calculated for the intervals $\pi < T < 2\pi$, $3\pi < T < 4\pi$, and $5\pi < T < 6\pi$. (d) The function $\tau_{c*}(\mu) = \min \tau_c(T)$ calculated separately for the same intervals.

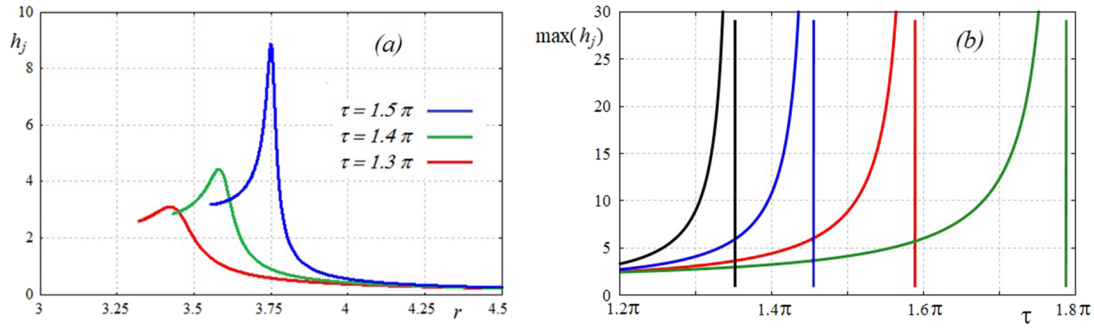

FIG. 5. (a) The thickness of the spray sheet as a function of the radial coordinate r at different time instants for $\mu = 0.5$ in the dimensionless variables. (b) The evolution of the maximum thicknesses of the spray sheet as functions of time for $\mu = 0.4$ (green line), $\mu = 0.5$ (red line), $\mu = 0.6$ (blue line), and $\mu = 0.7$ (black line). The vertical lines show the corresponding values of time τ_{c*} when the sheet thickness becomes unbounded.

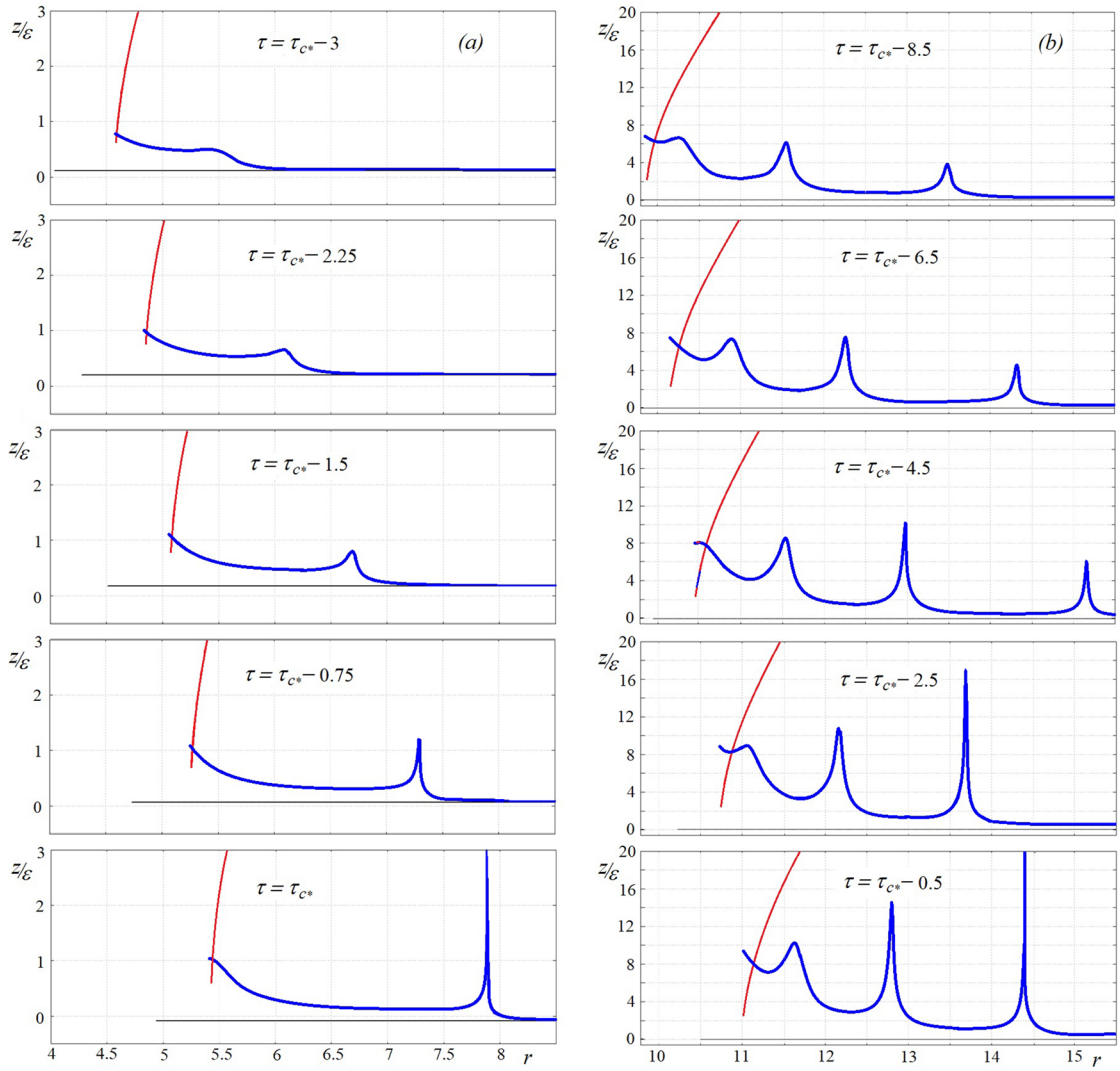

FIG. 6. Evolution of the spray sheet shown in the dimensionless variables by blue lines. The positions of the droplet free surface in the main flow region are shown by red lines. The black lines present the positions of the plate. (a) $\mu = 0.2$, $\varepsilon = 0.1$, ($\tau_{c*} = 9.86$, $r_{c*} = 7.88$); (b) $\mu = 0.05$, $\varepsilon = 0.1$, ($\tau_{c*} = 40.85$, $r_{c*} = 14.57$) [see Fig. 4(b)]. The jet root solution, which smoothly matches the free surfaces in the main flow region and in the jet sheet, is not shown.

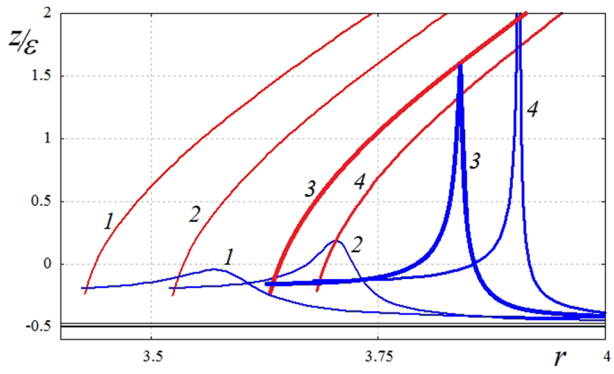

FIG. 7. Evolution of the spray sheet in the dimensionless variables (blue lines) and positions of the droplet free surface in the main flow region (red lines) for $\mu = 0.5$ ($\tau_{c*} = 4.99$, $r_{c*} = 3.9$) are shown in time instants $\tau = \tau_{c*} - 0.565$ (lines 1), $\tau = \tau_{c*} - 0.34$ (lines 2), $\tau = \tau_{c*} - 0.115$ (lines 3), and $\tau = \tau_{c*}$ (lines 4).

with splashing, if the flow in the normal to the plate direction occurs far enough from the contact region (see Fig. 6), or with air entrainment by the front of the advancing jet root region and subsequent discontinuity of the contact line velocity (see Fig. 7 for $\mu = 0.5$), where the splashing jet shown by line 3 impacts the main free surface of the droplet at time $\tau = \tau_{c*} - 0.115$ trapping the air.

V. DROP IMPACT ON ELASTICALLY SUPPORTED PLATE

It was shown in Sec. IV that plate vibration may lead to an unbounded increase of the spray sheet thickness. A liquid drop impact onto a rigid plate supported by a spring may cause vibration of the plate with a subsequent splashing or air entrainment. In this section, it will be shown that this scenario is impossible within the asymptotic model of drop impact employed in this study.

We consider a horizontal plate of mass m supported by a spring of rigidity k (see Fig. 8). A liquid drop of radius R and density ρ approaches the plate from above at speed V. The plate displacement

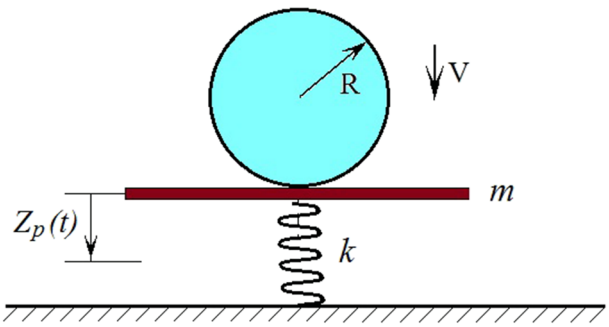

FIG. 8. Sketch of the drop impact on an elastically supported plate.

$Z_p(t)$ is governed by the following equation:

$$mZ_p'' + kZ_p = F(t), \qquad Z_p(0) = 0, \qquad Z_p'(0) = 0, \tag{18}$$

where $F(t)$ is the hydrodynamic force due to the drop impact [see Korobkin and Scolan (2006)],

$$F(t) = \frac{4}{3}\rho\,(3R)^{3/2}\frac{d}{dt}\left[Z_d^{3/2}(t)Z_d'(t)\right]. \tag{19}$$

$Z_d(t) = Vt - Z_p(t)$ is the displacement of the drop with respect to the moving plate. The plate [Eq. (18)] with the force (19) in the dimensionless variables,

$$Z_d = Az_d(\tau), \qquad \omega_0 t = \tau, \qquad \omega_0 = \sqrt{k/m},$$
$$A = (3m/4\rho)^{2/3}/(3R),$$

reads

$$\frac{d}{d\tau}\left[(1 + z_d^{3/2})z_d'(\tau)\right] + z_d(\tau) = \frac{\tau}{\nu} \qquad (\tau > 0),$$
$$z_d(0) = 0, \qquad z_d'(0) = \frac{1}{\nu}, \tag{20}$$

where $\nu = A\omega_0/V$. The solution $z_d(\tau)$ is determined numerically. The radius of the contact line is $R_c(t) = \sqrt{3RAz_d(\tau)}$. The unbounded growth of the spray sheet thickness is possible only if $R_c''(t) > 0$ at certain t, which provides

$$Q(\tau) = \frac{z_d(\tau)\tau}{\nu} - z_d^2(\tau) - 2z_d^{3/2}(z_d')^2 - \frac{1}{2}(z_d')^2 > 0. \tag{21}$$

The equation of the plate motion (20) was integrated in time for different values of the parameter ν. The maximum of $Q(\tau)$, where $0 < \tau < 10$, as a function of ν is shown in Fig. 9 for $0 < \nu < 10$. It is seen that $Q(\tau)$ is always negative. Therefore, the splashing induced by the plate vibration cannot be observed if the plate is supported by a spring. The minimum of the derivative $z_d'(\tau)$, which is proportional to the speed of the contact line, where $0 < \tau < 10$, as a function of ν is also shown in Fig. 9 for $0 < \nu < 10$. We conclude that the plate does not vibrate as a result of the drop impact for any rigidity of the supporting spring.

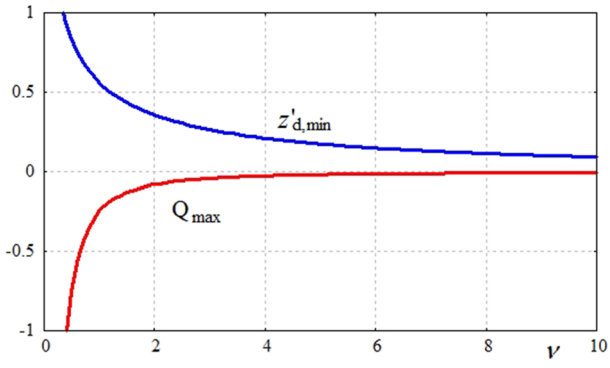

FIG. 9. The maximum of $Q(\tau)$ and the minimum of $z_d'(\tau)$ in the interval $0 < \tau < 10$ as functions of the parameter ν.

To compare our results, which were obtained for droplet impact onto a rigid plate vibrating at a given frequency ω with amplitude a in Sec. IV, and the same droplet impacting at the same speed V onto an elastically supported plate, as it is studied in this section, we select the parameters of the elastically supported plate such that the scale of the plate displacement A is equal to a and the natural frequency ω_0 is equal to ω. The conditions of calculations in Sec. IV, $\omega = 2\cdot10^{-5}$ s^{-1} and $a = 7\cdot10^{-6}$ m, and the equalities $A = a$ and $\omega_0 = \omega$ provide the mass of the plate $m = 4.2\cdot10^{-9}$ kg and the rigidity of the supporting spring $k = 168$ N/m. Then, the time scales are the same in both problems, $1/\omega$, and the parameter ν from Eqs. (20) is equal to μ, where the parameter $\mu = a\omega/V$ was defined in Sec. IV. To compare the present results with the results of Sec. IV, one should change the sign of the parameter μ, which is equivalent to the phase shift π of the plate vibration with respect to the impact instant. Note that the relative speed of impact on the vibrating plate at $t = 0$ is equal to $V(1 + \mu)$, but the relative speed of impact on the elastically supported plate is equal to V. Therefore, we cannot explicitly compare these two types of impacts for non-zero μ. For the stationary plate, $\mu = 0$. The relative speed of impact on the elastically supported plate is decreasing with time, which could be related to negative values of μ. The results of two problems are compared in terms of the acceleration of the contact region expansion in Fig. 10. It was shown in Sec. IV that the acceleration of the radius of the contact line, $R_c''(t)$, calculated within the Wagner impact model is responsible for possible splashing. The dimensionless accelerations, $R_c''(t)/[\omega\sqrt{RV\omega}]$, for the problem of forced plate vibration are equal to $r_c''(\tau)$, where $r_c(\tau)$ is given in (5),

$$\frac{R_c''(t)}{\omega\sqrt{RV\omega}} = \frac{\sqrt{3}}{4h^{3/2}}\left[2hh'' - (h')^2\right], \qquad h(\tau) = \tau + \mu\sin\tau. \tag{22}$$

This acceleration is shown in Fig. 10(a) for $\mu = 0$, 0.4, and 0.7. The importance of phase shift in the impact problem is demonstrated by Fig. 10(b), where $\mu = 0$, −0.4, and −0.7, which corresponds to the phase shift π of the plate vibration. The value $\mu = 0$ corresponds to the static plate without vibration. The phase shift is important during the first period of the plate vibration, $0 < \tau < 2\pi$, but then its effect is reduced to the change of sign of the acceleration [see also Eq. (7)]. The dimensionless accelerations,

$$\frac{R_c''(t)}{\omega\sqrt{RV\omega}} = \frac{\sqrt{3\nu}}{2z_d^{3/2}(1+z_d^{3/2})}Q(\tau), \tag{23}$$

for the problem of impact onto an elastically supported plate, where $A = a$, $\omega_0 = \omega$, and $\nu = \mu$, are shown in Fig. 10(c) for different values of the parameter ν. It is seen that the motions of the contact line with and without plate vibration are different in nature. There are some indications of oscillation of the acceleration for $0 < \tau < 3\pi$ in Fig. 10(c), but they do not lead to positive accelerations as in Figs. 10(a) and 10(b).

We can conclude that splashing caused by the plate vibration may occur only if the vibration is forced. Another option for vibration induced splashing is the plate of a small radius mounted in an otherwise rigid substrate. The latter problem was studied by Pegg *et al.* (2018) for an elastic simply supported circular plate. Our conclusion of no-splashing for impact onto an elastically supported plate is related only to a particular type of splashing studied in Sec. IV, which is caused by plate vibration and occurs during the early stage of the impact. We showed that the elastically supported plate does not oscillate during the early stage for any rigidity of the supporting spring (see the blue line in Fig. 9, which shows the relative velocity of the impact for a non-stationary plate). However, the motion of an elastically supported plate, which is caused by the droplet impact on it, reduces the relative speed of the impact and, therefore, reduces splashing of the droplet [see Rein (1993), Yarin (2006), and Howland *et al.* (2016) for more discussions of physics of splashing and comparison with experimental data].

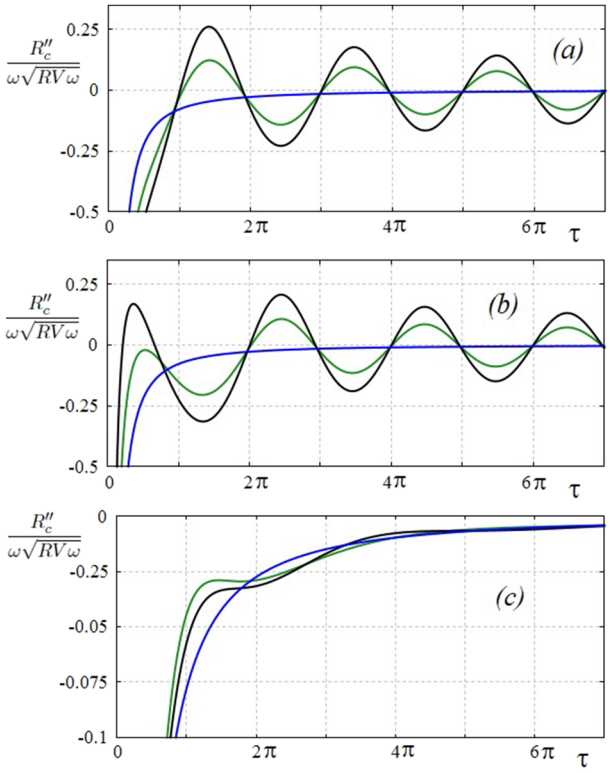

FIG. 10. Dimensionless accelerations of the contact region expansion for droplet impact on a stationary plate (blue line), (a) a vibrating plate with $\mu = 0.4$ (green line), 0.7 (black line); (b) a vibrating plate with $\mu = -0.4$ (green line), −0.7 (black line); and (c) an elastically supported plate with $\nu = 0.4$ (green line), 0.7 (black line).

Similar splashing jets may occur in the wake behind an elastic plate obliquely impacting onto a thin liquid layer [see Khabakhpasheva and Korobkin (2020)]. In this two-dimensional problem, the liquid is forced to flow from the region under the elastic plate into the wake at a relatively high speed, which may oscillate in time. If the flow from under the plate accelerates, a splashing jet emanated from the wake can be formed. The modeling of this splashing jet is similar to that of the present paper.

VI. CONCLUSION

It has been shown that, within the asymptotic theory of the early stage of the droplet impact at constant speed V, the pressure in the

contact region can be below the atmospheric pressure even for small amplitudes a of the plate vibration [see Fig. 3(a)]. The magnitudes of the negative pressures grow in time as the square root of time. For relatively large amplitudes a of the plate vibration with $a\omega/V < 1$, where ω is the frequency of the plate vibration, ventilation may occur with the zone of negative pressures approaching the periphery of the contact region and the air being sucked into the contact region. The effect of the phase shift of the plate vibration with respect to the impact instant was not taken into account in the present study. This effect could be important for splashing. The vibration of the plate affects the motion of the contact line between the plate and the free surface of the droplet. If the contact line accelerates, then the time and position of splashing are predicted by the equations of Sec. IV. The vibration of the plate increases the hydrodynamic force acting on the plate.

The obtained results and the employed theoretical model of the initial stage of drop impact are valid for certain ranges of the problem parameters. The amplitude a of the plate vibration should be much smaller than the length scale of the problem, L. Only in this case, the body boundary condition can be imposed approximately at the initial position of the plate, $z = 0$. The inequality, $a \ll L = \sqrt{RV/\omega}$, provides $a^2\omega \ll RV$ and $\mu \ll R/a$, which is satisfied in our analysis because $\mu < 1$ and $a \ll R$. The inequality $\mu < 1$ guarantees that the contact region monotonically expands in time. The time scale $1/\omega$ is assumed to be larger than the acoustic time scale, $t_{ac} = R/c_0$, where c_0 is the sound speed in the liquid. Here, t_{ac} is equal to the time traveled by acoustic waves from the place of the impact to the center of the drop. This condition yields $\omega \ll c_0/R$. In the example at the end of Sec. III with a water droplet of radius 1 mm, we have $c_0/R = 15 \cdot 10^5\ \mathrm{s}^{-1}$, which is larger than the frequency in that example. In addition, the impact speed V should be much smaller than the sound speed c_0 to justify the incompressible liquid model, $V \ll c_0$. We also require that the inequality $1/\omega \ll R/V$ is held, which implies that the drop displacement is much smaller than the radius R during the initial stage, the duration of which is of the order of $O(1/\omega)$. The incompressible and linear hydrodynamic model of this study can be used if

$$\frac{V}{R} \ll \omega \ll \frac{c_0}{R}.$$

The liquid viscosity can be neglected if the Reynolds number $Re = RV/\nu$, where ν is the kinematic viscosity of the liquid, is large. For a water droplet of radius 1 mm and impact speed 2 m/s, we find $Re = 2000$. Surface tension and gravity can be neglected during the early stage of the droplet impact onto the vibrating plate based on similar arguments as in Pegg *et al.* (2018).

The process of the droplet impact onto a vibrating rigid plate can be described by using the ideas from the water entry and exit model of Korobkin *et al.* (2017). During the first half of the first period of the plate vibration, $0 < \tau < \pi$, the relative speed of the drop with respect to the vibrating plate decreases from $V(1 + \mu)$ to $V(1 - \mu)$. This impact with deceleration leads to negative pressures in the contact region if $\mu > 1/5$. During this stage, the speed $R_c'(t)$ of the contact line is very high and the contact line acceleration is negative. During the second stage, $\pi < \tau < 2\pi$, the relative speed of the impact increases leading to positive loads on the plate and acceleration of the contact line. If $\mu > 1/5$, then this is the stage that determines the time and place of the blow-up of the spray sheet. During the following stages, with the duration π each in the dimensionless variables, we can distinguish the stage with positive and negative hydrodynamic loads and with positive and negative accelerations of the contact line. The magnitude of the loads increases in time. The derived asymptotic solution can be used only up to the first time instant of the spray sheet blow-up. This scenario of droplet impact could also be observed for a stationary plate with the droplet oscillating at a high frequency before the impact. The latter problem has not been studied yet.

Preliminary results of this paper were presented at the 3rd International Conference on Violent Flows (VF-2016), Osaka, Japan, 9–11 March 2016 (Khabakhpasheva and Korobkin, 2016); British Applied Mathematics Colloquium, Oxford, United Kingdom, 5–8 April 2016 (Korobkin and Khabakhpasheva, 2016); and 11th European Fluid Mechanics Conference, Sevilla, 12–16 September 2016.

AUTHORS' CONTRIBUTIONS

All authors contributed equally to this work.

ACKNOWLEDGMENTS

Preliminary theoretical results of this study were obtained within the project "Splashing on flexible substrates—a basic study" supported by The Royal Society of London, United Kingdom, and the National Science Council of Taiwan. Numerical analysis of splashing was performed, and conditions of air entrainment during the droplet impact were investigated under the support of the Russian Science Foundation, "The effect of air entrainment in oblique body impact on the liquid surface," Project No. 19-19-00287.

DATA AVAILABILITY

The data that support the findings of this study are available within the article.

REFERENCES

Courbin, L., Bird, J. C., and Stone, H. A., "Splash and anti-splash: Observation and design," Chaos **16**(4), 041102 (2006).

Chen, J. H., "Characteristics of drop impact on elastic and compliant surfaces," J. Mar. Sci. Technol. **13**, 156–161 (2005).

Faltinsen, O. M., "Hydroelastic slamming," J. Mar. Sci. Technol. **5**(2), 49–65 (2000).

James, A. J., Vukasinovic, B., Smith, M. K., and Glezer, A., "Vibration-induced drop atomization and bursting," J. Fluid Mech. **476**, 1–28 (2003).

Howison, S. D., Ockendon, J. R., and Wilson, S. K., "Incompressible water-entry problems at small deadrise angles," J. Fluid Mech. **222**(1), 215–230 (1991).

Howland, C. J., Antkowiak, A., Castrejon-Pita, J. R., Howison, S. D., Oliver, J. M., Style, R. W., and Castrejon-Pita, A. A., "It's harder to splash on soft solids," Phys. Rev. Lett. **117**(18), 184502 (2016).

Khabakhpasheva, T. I. and Korobkin, A. A., "Liquid drop impact on a vibrating substrate," in Proceedings of 3rd International Conference on Violent Flows (VF-2016), Osaka, Japan, 9–11 March 2016.

Khabakhpasheva, T. I. and Korobkin, A. A., "Oblique elastic plate impact on thin liquid layer," Phys. Fluids **32**(6), 062101 (2020).

Korobkin, A. A., *Liquid-Solid Impact* (Siberian Branch of the Russian Academy of Sciences, Novosibirsk, 1997).

Korobkin, A. A., "Wave impact on the center of an Euler beam," J. Appl. Mech. Tech. Phys. **39**(5), 134–147 (1998).

Korobkin, A. A. and Khabakhpasheva, T. I., "Regular wave impact onto an elastic plate," J. Eng. Math. **55**(1-4), 127–150 (2006).

Korobkin, A. and Khabakhpasheva, T., "Effect of vibrations on liquid drop impact," in Book of Abstracts BAMC, Oxford, United Kingdom, 5–8 April 2016 p. 139, available at https://docs.google.com/viewer?a=v&pid=sites&srcid=ZGVmYXVsdGRvbWFpbnxiYW1jMjAxNm94Zm9yZHxneDoyOTM-2ZGE5Yjk2OWJhNjE3.

Korobkin, A. A., Khabakhpasheva, T. I., and Maki, K. J., "Hydrodynamic forces in water exit problems," J. Fluids Struct. **69**, 16–33 (2017).

Korobkin, A. A., Khabakhpasheva, T. I., and Wu, G. X., "Coupled hydrodynamic and structural analysis of compressible jet impact onto elastic panels," J. Fluids Struct. **24**(7), 1021–1041 (2008).

Korobkin, A. A. and Pukhnachov, V. V., "Initial stage of water impact," Annu. Rev. Fluid Mech. **20**(1), 159–185 (1988).

Korobkin, A. A. and Scolan, Y.-M., "Three-dimensional theory of water impact. Part 2. Linearized Wagner problem," J. Fluid Mech. **549**, 343–373 (2006).

Moradi, M., Rahimian, M. H., and Chini, S. F., "Numerical simulation of droplet impact on vibrating low-adhesion surfaces," Phys. Fluids **32**(6), 062110 (2020).

Oliver, J. M., "Water entry and related problems," Ph.D. thesis, University of Oxford, 2002.

Pegg, M., Purvis, R., and Korobkin, A. A., "Droplet impact onto an elastic plate: A new mechanism for splashing," J. Fluid Mech. **839**, 561 (2018).

Pepper, R. E., Courbin, L., and Stone, H. A., "Splashing on elastic membranes: The importance of early-time dynamics," Phys. Fluids **20**(8), 082103 (2008).

Rein, M., "Phenomena of liquid drop impact on solid and liquid surfaces," Fluid Dyn. Res. **12**(2), 61 (1993).

Scolan, Y.-M. and Korobkin, A. A., "Energy distribution from vertical impact of a three-dimensional solid body onto the flat free surface of an ideal fluid," J. Fluids Struct. **17**(2), 275–286 (2003).

Tsai, P. H., Wang, C. H., Wang, A. B., Korobkin, A., Purvis, R., and Khabakhpasheva, T., "Investigation of droplet oscillation on a vibrating elastic plate," in *13th Asian Symposium on Visualization, Novosibirsk, Russia, June 22-26 2015* (Parallel, Novosibirsk, 2015), p. 9.

Wagner, H., "Über stoß- und gleitvorgänge an der oberfläche von flüssigkeiten," ZAMM **12**(4), 193–215 (1932).

Yarin, A. L., "Drop impact dynamics: Splashing, spreading, receding, bouncing...," Annu. Rev. Fluid Mech. **38**, 159–192 (2006).